Multivariate Statistical Evaluation of Multielement Geochemical Dataset from the Recsk Deep Porphyry-Skarn Deposit

DIM-ESEE Conference
21st – 23rd October 2026, Zagreb, Croatia
DOI: 10.17794/dimesee.2026.2.2

Anthonio Edhy Florice Solonandrasana[1], Ferenc Mádai[1*]
[1] University of Miskolc, H-3515 Miskolc-Egyetemváros, Hungary

Abstract

The Recsk Deep deposit in northern Hungary represents a complex porphyry–skarn–epithermal mineral system with notable critical raw material potential. This study examines minor- and trace-element associations in 66 archived samples representing Diorite, Skarn, and Carbonate lithologies. Pearson correlation networks, principal component analysis, and K-means clustering were applied to characterize elemental relationships and lithological controls. A consistently strong Mo–Re association was identified across all lithologies, whereas polymetallic element associations display pronounced lithology-dependent variations. Carbonate rocks show high degree of elemental correlations, suggesting enhanced metal mobility and redistribution, however, due to low sample numbers this is not fully reliable. Findings demonstrate the key influence of host-rock composition and fluid–rock interaction on the geochemical architecture of the Recsk mineral system.

Keywords: Recsk Hungary, porphyry-skarn deposit, multielement geochemistry.

1. Introduction

The Recsk ore deposit, located in the Mátra Mountains of northern Hungary, represents one of the most significant porphyry-related mineral systems in Central Europe. It is a concealed porphyry copper–molybdenum (Cu–Mo) system associated with Miocene calc-alkaline magmatism and forms part of the Neogene metallogenic evolution of the Carpathian–Pannonian region (**Szabó et al., 1992**). The deposit exhibits complex vertical and lateral metal zonation, comprising a deep porphyry Cu–Mo system overlain by skarn and epithermal mineralization.

Within the Recsk ore field, Miocene intermediate intrusive bodies were emplaced into a heterogeneous basement composed of Mesozoic carbonate sequences and older volcanic formations. Interaction between the magmatic–hydrothermal system and the reactive carbonate host rocks played a fundamental role in controlling metasomatic processes and the development of hydrothermal mineralization (**Biró et al. 2024**). Regional fault systems provided structural pathways for magma ascent and subsequent hydrothermal fluid circulation, thereby influencing the spatial distribution of alteration zones and mineral assemblages.

The significance of the Recsk deposit lies not only in its copper and molybdenum potential but also in its scientific value as a well-studied example of a telescoped porphyry–skarn–epithermal system. Mineralization is hosted primarily by andesitic to dioritic intrusive bodies and the surrounding carbonate country rocks, where contact metasomatism and hydrothermal alteration produced extensive skarn assemblages (**Biró et al. 2024**). Fig. 1. shows the general structure of the complex along a WSW-ENE section (K-14) compiled by **Biró et al. (2024)**.

The principal exploration phase of the Recsk Deep deposit took place between the 1960s and 1980s and led to the recognition of a concealed porphyry–skarn mineralization system beneath the Lahóca area (**Baksa et al. 1980**). Extensive geological, geophysical, and drilling campaigns were subsequently conducted to investigate the geometry, continuity, and economic potential of the deep orebody. During this period, several important geological and mineralogical studies substantially advanced the understanding of the Recsk porphyry–skarn system. The study by **Baksa et al. (1980)** provided detailed interpretations of the geological structure, hydrothermal alteration, and mineralization characteristics of the deposit, while **Csillag (1975)** described the magmatic-related alteration assemblages within the Recsk complex.

Most recently, **Biró et al. (2023)** investigated trace-element distributions in sulphide minerals using modern analytical techniques and demonstrated that the Recsk deposit contains enrichments in elements associated with critical raw materials (CRMs), including PGE. **Biró et al. (2024)** further refined the interpretation of CRM-bearing mineralization by integrating modern geochemical data with archived exploration materials, emphasizing the potential economic and scientific significance of CRM-related elements within the Recsk porphyry–skarn system. Their study demonstrated that molybdenite associated with porphyry mineralization contains the highest Re concentrations, whereas Ag, Bi, Se, Sb, and Zn become progressively enriched toward distal carbonate-replacement mineralization.

The Recsk Deep (Recsk II) mining plot has had temporarily suspended status since 2000, and its underground shafts and galleries are currently flooded. Nevertheless, the National Exploration Plan prepared in accordance with the EU

*Corresponding author: Ferenc Mádai
e-mail address: ferenc.madai@uni-miskolc.hu

Critical Raw Materials Act in 2025 identified the Recsk complex as Hungary's highest-priority target for mineral exploration and future mine development (**SARA, 2026**).

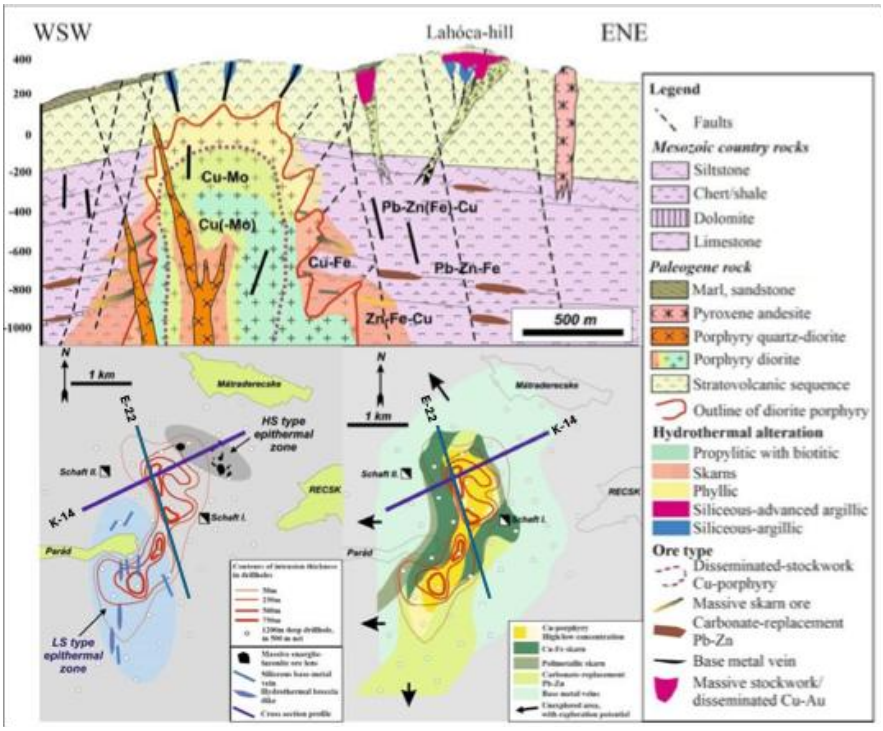


Figure 1. Cross-section of Recsk's local geological Setting (**Biró et al., 2024**) with the projections of cross sections K-14 and E-22.

2. Methods

A project entitled *Development of the Geochemical Database of the Recsk Deep Level and Re-evaluation of the Geomodel Using 3D Modelling* was initiated by the Institute of Exploration Geosciences at the University of Miskolc and Nitrokémia Zrt., the state-owned company responsible for supervising Hungary's legacy mining sites. The work undertaken in 2025 aimed to improve and expand the digitized geological and geochemical databases of the Recsk Deep deposit and to generate new analytical data from archived materials - including drill cores, polished sections, and thin sections - using advanced analytical techniques. Investigations focused on two geological cross-sections, E–22 and K–14.

The project was conducted jointly by the Institute of Exploration Geosciences at the University of Miskolc and the Department of Mineralogy, Institute of Geography and Earth Sciences, Eötvös Loránd University (ELTE), Budapest. One of its principal objectives was to develop an updated alteration model for the deep part of the Recsk complex based on new geochemical, mineralogical, and petrographic data obtained along the two cross-sections. The model was developed using XRF and XRD data from 160 samples, complemented by detailed petrographic analyses of thin and polished sections. Based on these results, alteration facies and alteration types were identified and delineated, following the systematics of **Large (2025)** and **Bouzari et al. (2022)**.

Work Package 3 focused on the minor- and trace-element characteristics of the deposit, using new, high-quality analytical data to assess its critical raw material potential. Of the 160 selected samples, 66 were analysed for 40 geochemical variables by ALS Global using ICP–MS following four-acid digestion.

The element association presented in this study is derived from a geochemical dataset used to construct correlation network diagrams based on strong relationships between elements. The dataset consists of 66 archived samples selected from the Recsk cross-sections K-14 and E-22, which were submitted for modern geochemical analysis at ALS Laboratories using ICP-MS coupled with four-acid digestion. The resulting network diagrams provide an integrated overview of geochemical relationships and elemental associations within the Recsk deposit across the investigated lithologies. Based on WDXRF major element geochemical data, observations of existing thin sections and polished sections, three major lithologic groups were defined: 1.) main volume of the diorite - quartz diorite intrusion, 2.) skarn bodies along the border of the intrusion and host rocks, and 3.) carbonate-rich rocks of the Mesozoic sequence.

Analysed samples are distributed as follows among lithology types and cross sections: Diorite lithology – 33 samples (14 along K-14, 19 along E-22), Skarn lithology – 29 samples (9 along K-14, 20 along E-22), Carbonate lithology – 4 samples (3 along K-14, 1 along E-22). Samples for ICP-MS analysis were selected on a multiple set of criteria: having archive whole rock chemistry data (6), having archive Au assay data (28), additionally by structural position from Rm-

series drillholes started from surface (19), by structural position from F-series drillholes started from underground workings at -700 and -900 m (13).

To evaluate elemental relationships, Pearson correlation coefficients (*r*) were calculated between the analysed elements using the geochemical dataset in Excel. The resulting correlation matrix was subsequently used to construct correlation network diagrams, where nodes represent individual elements and connecting lines represent statistically significant positive correlations above the selected threshold value (above 0.6). Then, correlation between 0.6 to 0.8 was classified as strong and over 0.8 as very strong. The network diagrams were generated using a python force-directed automatic clustering layout (igraph software package), in which strongly correlated elements are grouped closer together, while weakly related elements are positioned farther apart (**Csardi and Nepusz, 2006**). This clustering approach allows the identification of geochemical associations and elemental groups sharing similar geochemical behaviour or mineralogical affinity (**Reimann et al., 2008**).

In addition to the cross-correlation network diagram, Principal Component Analysis (PCA) was required to further understand the distribution and association of chemical elements within the Recsk ore system. The PCA method was applied separately to different lithological datasets, using the same ALS geochemistry data. Prior to PCA calculation, the geochemical dataset was standardized to minimize the influence of differences in elemental concentration ranges. The PCA was then performed using the correlation matrix of the standardized variables. The first two principal components (PC1 and PC2), representing the highest proportion of variance within each dataset, were selected for visualization in two-dimensional PCA diagrams. To further distinguish elemental associations, K-means clustering was applied to the PCA results using data analysis tools of the ioGAS 8.2 software. The optimal number of clusters for each lithology was determined using Silhouette score evaluation, allowing the identification of the most statistically coherent elemental groupings. The resulting PCA clustering diagrams provide a visual representation of geochemical affinities and elemental distribution patterns within the Recsk system (**Reimann et al., 2008**).

3. Results

In the Diorite lithology, the cross-correlation network diagram (**Figure 2a**) shows a well-defined clustering of elements, with positive correlations. A prominent feature is the dense cluster formed by Pb-Zn-Cd-Ag-Bi-Sb-Se-Te, where numerous very strong correlations create a highly interconnected group. Some associations observed generally over the analysed samples, such as the Mo-Re, Zr-Hf pairs, are clearly expressed in all three lithologies.

The PCA diagram of the Diorite lithology (**Figure 2b**) shows some well-defined elemental clusters. Like in the correlation network diagram, a compact group composed of Pb-Bi-Te-Se-Ag-Zn (Cluster 3) is clearly distinguished in the PC1-PC2 space, corresponding to the strongly interconnected polymetallic cluster identified in the correlation network. Similarly, Cu, Mo, In, and Sn form a separate cluster (Cluster 5) within the PCA diagram. Additional clusters are also visible in the PCA diagram, including groups dominated by Ti-Sc-Y-Na (Cluster 6) and Fe-Co-Ni-Cr-W (Cluster 1) associations.

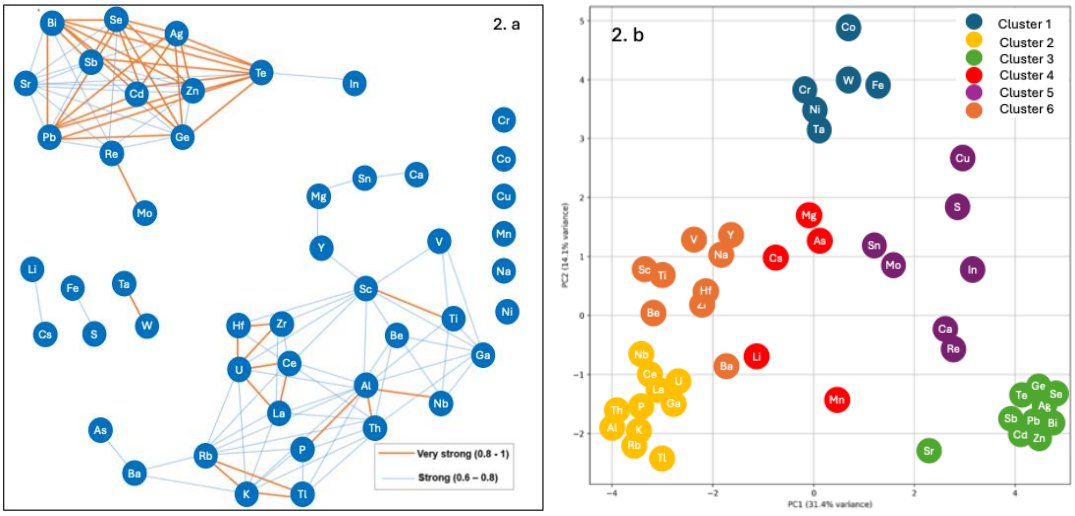


Figure 2. Clustering diagrams for the Diorite lithology, (a) correlation network diagram, (b) PC1-PC2 plot.

Statistical test shows for the Diorite lithology an internal geochemical heterogeneity, silhouette scores indicate relatively weak cluster simulation. This can be a result of multiply alteration events which affected the dioritic intrusive body. Multivariate homogeneity test proves the inhomogeneity of the sample population.

The Skarn lithology reveals several distinct element groupings defined by strong correlation. A notable feature of cross-correlation network diagram (**Figure 3a**) is the development of a compact cluster, involving Pb-Sb-As-Cs-Li, and numerous very strong correlations between these elements. In addition, elements such as Zn-Ag-Cd-Ce, K-Rb-Ba-Tl, Ti-Al-P-Sc-Be form smaller interconnected groups, characterized by both strong and very strong correlations.

The skarn diagram displays a shift in the distribution of correlations, with several associations becoming more localized. The Mo-Re relationship looks closer in the Skarn lithology compared to diorite, which indicates the better incorporation of Re in molybdenite in skarns.

The PCA diagram of the Skarn lithology (**Figure 3b**) shows agreement with the principal associations identified in the correlation network diagram. Several compact elemental clusters are clearly distinguished within PC1-PC2 space. A prominent cluster composed of Pb-Sb-As-Cs-Li (Cluster 5) is particularly well defined, consistent with the dense interconnected relationships observed in the correlation network.

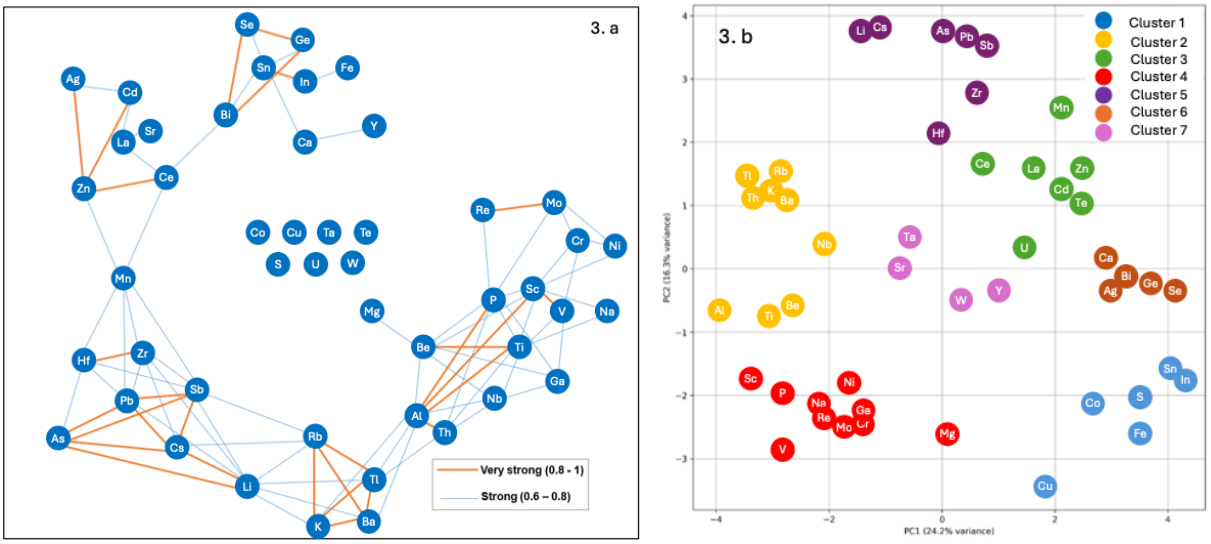


Figure 3. Clustering diagrams for the Skarn lithology, (a) correlation network diagram, (b) PC1-PC2 plot.

The PCA diagram also highlights additional elemental associations, in particular, the Rb-K-Ba-Tl association, which forms a distinct cluster within the PC1-PC2 space, while elements related to the Ti-Al-Th-Be system are also grouped together. The PCA diagram shows a stronger separation between lithology-related element groups and polymetallic associations. Additional clusters involving Zn-Mn-La-Ce (Cluster 3) and Fe-Co-In-Sn (Cluster 1) are also visible within the PCA diagram, further emphasizing the complexity of elemental distribution within the Skarn lithology.

Statistical test for the Skarn lithology shows some evidence of internal geochemical heterogeneity. Separation of the clusters are relatively weak, subpopulations are not statistically robust. In the Skarn lithology exo-, endo-, and aposkarn samples are grouped, which contributes to these statistical test results.

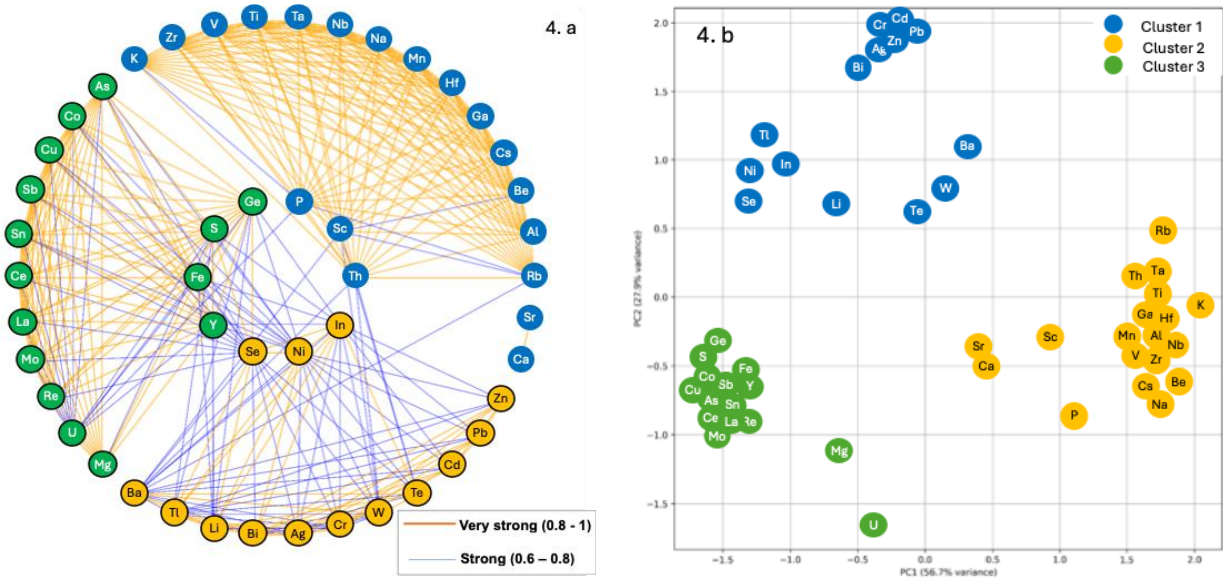


Figure 4. Clustering diagrams for the Carbonate lithology, (a) correlation network diagram, (b) PC1-PC2 plot.

In the Carbonate system, a remarkable feature is the apparent extensive connectivity within groups such as Zr, V, Ti, Nb, Na, Mn, and Hf, where a dense network of very strong correlations forms a broad and cohesive cluster. Similarly, elements including Ce, La, Sn, Sb, Cu, Co, and Mo are linked through multiple very strong associations, contributing to the overall complexity of the diagram.

 DOI: https://doi.org/10.17794/dimesee.2026.2.2

In comparison with the Diorite and Skarn lithologies, the carbonate network diagram (**Figure 4a**) shows a more continuous and less fragmented pattern, with fewer isolated clusters (only Ca-Sr) and a greater number of inter-element connections. Strong correlations are observed among elements such as Pb, Zn, Cd, and Te, forming a localized grouping within the broader network.

Like the correlation network diagram of the Carbonate lithology, the PCA diagram (**Figure 4b**) highlights also a high degree of interconnection between elements, reflected by the distribution of elemental associations within the PC1-PC2 space. Three distinct principal clusters can be clearly identified in both diagrams. The first cluster is dominated by Pb-Zn-Cd-Te associations (Cluster 1), corresponding to the polymetallic association observed in the correlation network diagram, while the second cluster includes Zr-V-Ti-Nb-Na-Mn-Hf (Cluster 2). A third localized grouping is represented by Ce-La-Sn-Sb-Cu-Co-Mo (Cluster 3). The Mo–Re association does not appear as an isolated pair but is integrated into a larger elemental cluster. Compared to the Diorite and Skarn datasets, the carbonate PCA displays a more continuous distribution of elements and fewer isolated clusters, reflecting the highly interconnected pattern observed in the carbonate correlation network. These more interconnected correlation patterns of the Carbonate lithology appear as the effect of the small number of available samples, thus the clusters and correlations are not approved by statistical tests.

4. Discussion

Correlation network analysis indicates a structured yet heterogeneous organization of elemental associations. A consistent feature throughout the entire dataset is the strong Mo-Re correlation (*r* values: 0.81 in diorite, 0.85 in skarn, 1.00 in carbonate), which is characteristic of porphyry-related mineral systems and reflects a genetic link to magmatic-hydrothermal processes. This association supports the interpretation of a high-temperature metal source related to intrusive activity (**Sillitoe, 2010**). The interpretation is further supported by recent geochemical investigations at Recsk that documented substantial Re enrichment in molybdenite and highlighted the close genetic relationship between Mo and Re within the porphyry environment (**Biró et al., 2024**).

In contrast, the distributions of other elements do not define a single, systematically organized clustering pattern but instead exhibit variable, lithology-dependent associations. Elements such as Cu, Zn, Pb, Sb, and As display differing degrees of correlation depending on host-rock lithology, as demonstrated by the distinct network structures observed in Diorite, Skarn, and Carbonate units. Element pairs with high correlation coefficient at least in one lithology group are shown in Table 1. The Carbonate lithologies exhibit a notably higher degree of correlations (see **Table 1.**), that might indicate enhanced metal mobility and redistribution within these chemically reactive host rocks. These results are in line with mass transfer calculation results completed on the same dataset (unpublished internal report). However, the high degree of correlation in Carbonates is an effect of the small number of samples in the analysed pool and are not validated by statistical tests. Recsk-specific geochemical studies demonstrate that trace-element signatures differ substantially among porphyry, skarn, and carbonate-replacement mineralization styles because of fluid evolution and metal redistribution (**Biró et al., 2024**).

Table 1. Correlation heatmap showing the variation in correlation (by correlation coefficient *r*) for selected element pairs across the Diorite, Skarn, and Carbonate lithologies of the Recsk deposit (red – very strong, green – weak).

Mo-Re	0.81	0.85	1.00
Pb-Zn	1.00	0.32	1.00
Zn-Cd	0.85	1.00	1.00
Cu-Mo	0.08	0.12	0.99
Sb-As	0.28	0.94	1.00
Zr-Hf	0.98	0.97	0.99
	Diorite	Skarn	Carbonate

The Diorite lithology exhibits more compact and well-defined clusters, reflecting more coherent elemental associations. This pattern is interpreted as evidence that the primary magmatic geochemical signature is comparatively well preserved, particularly for relatively immobile elements such as Ti, Zr, and Nb, as well as rare earth elements (e.g., La and Ce), with limited overprinting by later hydrothermal processes. Consequently, elemental relationships within the diorite remain relatively stable and systematically organized compared with those observed in more reactive lithologies. However, the effect of later alteration phases is reflected by statistical tests, weakening the evidence of statistically distinct, stable geochemical subpopulations.

5. Conclusions

Interpreted results were integrated with published literature on porphyry-skarn systems (**Einaudi et al., 1981; Sillitoe, 2010; Xiao et al., 2021**), allowing the construction of a conceptual diagram, to illustrate element mobility and redistribution within the Recsk deposit (**Figure 5**).

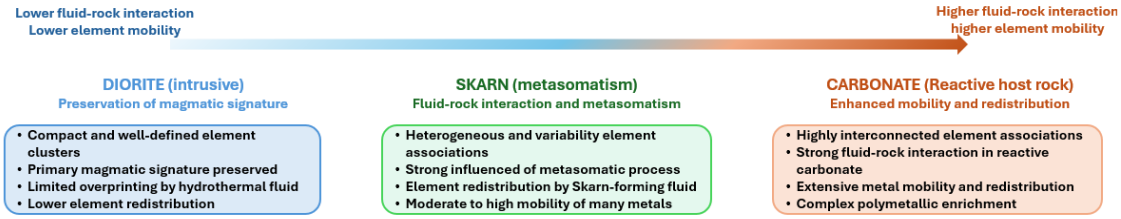


Figure 5. Conceptual model illustrating element mobility and redistribution within the Recsk porphyry-skarn system according to lithology. (modified after **Sillitoe, 2010; Einaudi et al., 1981; Xiao et al., 2021**).

Unlike many classical porphyry systems, in which elemental distributions are controlled primarily by proximity to the causative intrusion, the Recsk deposit exhibits a more complex geochemical architecture governed by the combined effects of hydrothermal evolution, host-rock composition, fluid–rock interaction, and metasomatic processes (**Figure 5**). This behaviour is consistent with porphyry–skarn systems in which elemental mobility and distribution are strongly influenced by fluid–rock interactions and the reactivity of the host lithologies (**Xiao et al., 2021**).

6. References

Baksa, Cs., Cseh Németh, J., Csillag, J., Földessy, J., Zelenka, T. (1980). The Recsk porphyry copper deposit, Hungary. In: Jankovic, S. & Sillitoe, R. (eds): *European Copper Deposits.* Beograd, 73–76.

Biró, M., Molnár, F., O'Brien, H. (2023). Occurrence of native platinum and PGE-bearing pyrite in the porphyry-skarn-epithermal ore complex at Recsk, Hungary. *Földtani Közlöny*, 153(3), pp. 261–264. https://doi.org/10.23928/foldt.kozl.2023.153.3.261

Biró M., Raith J.G., Feichter M., Hencz M., Gabriella B. Kiss,Virág A., Molnár F. (2024). Comparative Study of Sulfides from Porphyry, Skarn, and Carbonate-Replacement Mineralization at the Recsk Porphyry-Mineralized Complex, Hungary. *Minerals*, 14(9), 956. https://doi.org/10.3390/min14090956

Bouzari, F., Lee, R.G., Hart, C.J.R., van Straaten, B.I. (2022). Porphyry Vectoring Techniques in Advanced Argillic Altered Rocks of British Columbia: Geoscience BC Report 2022-03, MDRU Publication 456, 38 p.

Csardi, G., Nepusz, T., (2006). The igraph software package for complex network research. *InterJournal, Complex Systems*, 1695, pp.1–9. https://igraph.org/

Csillag, J. (1975). A recski terület magmás hatásra átalakult képződményei. *Földtani közlöny*, 105, p. 646–671.

Einaudi, M.T., Meinert, L.D. and Newberry, R.J. (1981). Skarn deposits. in Skinner B.J. (ed.) *75th Anniversary Volume*, Economic Geology Publishing Company, pp. 317–391. https://doi.org/10.5382/AV75.11

Large, R. R. (2025). Simple graphical tools to understand the relationship between porphyry composition, hydrothermal alteration, mineralogy and copper-gold grades in porphyry copper deposits. *Ore Geology Reviews*, 182, https://doi.org/10.1016/j.oregeorev.2025.106581

Reimann, C., Filzmoser, P., Garrett, R.G. and Dutter, R., (2008). *Statistical Data Analysis Explained: Applied Environmental Statistics with R.* Chichester: Wiley

Sillitoe, R.H., (2010). Porphyry Copper Systems. *Economic Geology*, 105, 3–41.

Supervisory Authority for Regulatory Affairs (SARA) (2026). National Exploration Programme, Hungary. https://hugeo.hu/sites/default/files/2026-06/CRM_HU_NEP_EN_v2.pdf

Szabó, Cs., Harangi, S. and Csontos, L. (1992). Review of Neogene volcanism of the Carpathian–Pannonian region. *Tectonophysics*, 208, pp. 243–256. https://doi.org/10.1016/0040-1951(92)90347-9

Xiao, Q., Zhou, T., Hollings, P., Wang, S., Liu, J., White, N. Fu, B. (2021). The role of porphyry-related skarns in the Chating porphyry copper and gold deposit, eastern China'. *Ore Geology Reviews*, 133, https://doi.org/10.1016/j.oregeorev.2021.104096 .

Acknowledgment

Authors acknowledge the background conceptual research of Ferenc Molnár, Máté Biró, Gabriella B. Kiss (ELTE) on delineating mineral alteration types and facies.

Funding

This research was funded by Nitrokémia Zrt. Hungary in 2025.

Author's contribution

Anthonio Edhy Florice Solonandrasana (MSc student) formal analysis, writing - original draft. **Ferenc Mádai** (Associate Professor, PhD): conceptualization, supervision, writing – review and editing.

All authors have read and agreed to the published version of the manuscript.